

Synthesis, characterisation, antimicrobial activity and DNA cleavage of (E)-4-[(2-Morpholinoquinolin-3-YL)Methaylene Amino] Phenol Schiff base metal complexes

Ambala Anilkumar and Ch. Abraham Lincoln*

Department of Chemistry, Osmania University, Hyderabad-500 007, INDIA

*lincoln.ab86@gmail.com

Abstract

A series of novel (E)-4-(((2-Morpholinoquinolin-3-yl)methaylene)amino)phenol Cu(II), Co(II), Ni(II), Zn(II) and Mn (II) metal complexes have been synthesized 1:1 metal to ligand ratio and these complexes were characterized by using analytical data such as FT-IR, UV-visible, Mass spectroscopy, SEM, EDX, TGA and magnetic moment measurements. The ligand and all the metal complexes were tested in vitro antimicrobial activity and DNA cleavage studies.

Keywords: Morpholie, Quinoline, Schiff base, Antimicrobial activity, DNA cleavage studies.

Introduction

Quinoline derivative are important antimalarial agents and possess other biological activities such as antimicrobial¹, antiproliferative², antimycobacterial³, antimalarial⁴, antitumor⁵, anti-inflammatory⁶, antiparasitic⁷, anti-HIV⁸, insecticidal⁹, antidyslipidemic and antioxidant¹⁰ activities. In addition, piperidine ring derivatives are considered as pharmaceutically important biologically active compounds used as vitamins, hormones and antibiotics¹¹⁻¹³. Morpholine nucleus is an important core of many drug molecules and also responsible for varied pharmacological activities like antihistamines, anticancer and antimicrobial activity.

Furthermore, Schiff bases are important classes of ligands which coordinate with metal ions via azomethine nitrogen and have been studied extensively due to their promising role in biological system¹⁴. On the other hand, several Schiff bases show broad range of pharmacological activities including antimicrobial, anti-malarial and anti-viral agents as well as the anti-inflammatory, antioxidant and anti-cancerous agents^{15,16}.

In view of the above findings we have synthesized the novel Schiff base ligand (E)-4-(((2-Morpholinoquinolin-3-yl)methaylene)amino)phenol and its bivalent metal complexes of Mn(II), Cu(II), Co(II), Ni(II) and Zn(II). The ligand and their metal complexes were characterized by various spectroscopic techniques and their antimicrobial activity and DNA cleavage studies were also reported.

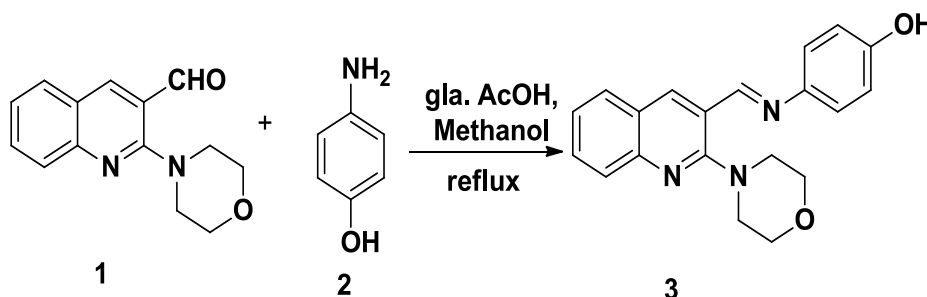
Material and Methods

Materials: All the chemicals were purchased from Sigma Aldrich. The solvents and reagents used were of analytical grade.

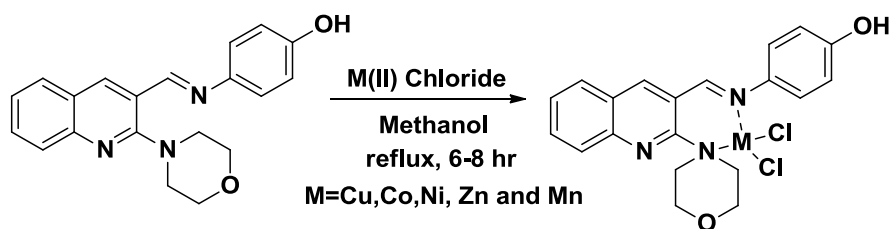
Synthesis of (E)-4-(((2-Morpholinoquinolin-3-yl)methaylene)amino)phenol (ligand) (3): A solution of 2-morpholinoquinoline-3-carbaldehyde (1) (5 mmol), 4-aminophenol (2) (5 mmol) in methanol was taken into round bottom flask and slowly catalytic amount of glacial acetic acid was added to the reaction mixture, then it was refluxed with continuous stirring for 1 hr. The reaction completion was checked by TLC. After completion of the reaction, observe the formation of light yellow precipitate, the precipitate was filtered, dried and recrystallised from EtOH to afford 82% of pure (E)-4-(((2-morpholinoquinolin-3-yl)methaylene)amino)phenol (3).

Synthesis of metal complexes: A methanolic solution of Metal (II) (Cu, Co, Ni, Zn and Mn) chlorides (5 mmol) was slowly drop by drop added to hot methanolic solution of (E)-4-(((2-Morpholinoquinolin-3-yl)methaylene)amino)phenol (5 mmol) at a metal to ligand ratio of 1:1.

After completion of addition, the resulting mixture was refluxed for 6 hr. The absence of ligand was checked by TLC, then it was cooled to room temperature and solvent evaporated under reduced pressure. The crude product was washed with hot methanol to yield amorphous metal complexes.



Scheme 1: Synthesis of (E)-4-(((2-morpholinoquinolin-3-yl)methaylene)amino)phenol (3)



Scheme 2: Synthesis of (E)-4-(((2-morpholinoquinolin-3-yl)methylene)amino)phenol metal complexes.

Physical measurement: The purity of the compound was checked by TLC using precoated silica gel plates 60₂₅₄(Merck). FTIR (KBr) spectra were recorded on a Shimadzu FT-IR-8400s spectrophotometer. ¹H NMR and ¹³C NMR spectra were recorded on Bruker Avance II 400 MHz spectrometer using tetramethylsilane as an internal standard. Mass spectra were recorded on ESI mass spectrometer. Elemental analysis was determined by using a Perkin /elmer 240(USA) CHNS analyzer. The electronic spectra of ligand and its complexes were carried out in DMSO using a SHIMADZU UV-2600 spectrophotometer. \

Thermo gravimetric analysis of the metal complexes was carried on a Shimadzu TGA-50H thermal analyzer in the temperature range of ambient temperature to 1200 °C with a heating rate of 10 °C min⁻¹. A Gouy balance model 7550 using [Co(NCS)₄] as standard is operated to examine the magnetic moment values of the metal complexes. The SEM/EDX images were obtained from Hitachi SEM analyser.

Antimicrobial activity

Antibacterial activity: The ligand and metal complexes were screened for their *in vitro* antibacterial activity against *Bacillus faecalis*, *Staphylococcus aureus*, *Klebsiella pneumonia* and *Escherichia coli* using ampicillin as standard drug. The activity was determined using cup plate agar diffusion method by measuring the zone of inhibition in mm. The complexes were screened at the concentration of 500µg/ml in DMSO.

Antifungal activity: The ligand and metal complexes were screened for their antifungal activity *in vitro* against *A. Niger* and *F. Oxysporum* using Grieseofulvin as standard drug. The activity was determined using cup plate agar diffusion method by measuring the zone of inhibition in mm. The complexes were screened at the concentration of 500µg/ml in DMSO.

DNA cleavage studies: The compounds were dissolved in DMSO, then added separately to the pUC18 DNA sample and H₂O₂. The sample mixtures were incubated at 37°C for 1 hour. The electrophoresis of the samples was done according to the following procedure. Weigh 0.25grams of agarose and dissolve it in 25 ml of 1x TAE buffer (121.1g Tris base, pH 8.0, 0.5 M EDTA, 57.1ml of Glacial acetic acid for 1 ltr) by boiling. When the gel attains approximately 55°C, pour it into the gel cassette fitted with comb gets solidified.

Carefully remove the comb, place the gel in the electrophoresis chamber flooded with TAE buffer. Load DNA sample with bromophenol blue carefully into the wells along with standard DNA marker and pass the constant 100 V of electricity till the dye front reaches to the end of gel. Remove the gel carefully stains with ETBR solution (10µg/ml) for 10-15 min. and observe the bands under UV transilluminator.

Results and Discussion

Physical characteristics of the complexes: All the metal complexes were colored, insoluble in water and melt at high temperature, non-hygroscopic in nature.

Elemental analysis: The percentage of the elements (C, H, N) present in the ligand and complexes was given in table 1 The experimental values matched with the theoretical values and these results confirmed 1:1 metal to ligand ratio. The values shown in brackets are calculated.

Mass spectra: The mass spectrum of the ligand and their metal complexes exhibits the molecular ion peak at (m/z), which is in agreement with its formula weight. The mass spectral values of the metal complexes were given in table 2.

NMR spectrum of ligand: The ¹H-NMR spectra of the ligand shows a singlet at δ 8.71 ppm assigned to azomethine proton integrated for one proton and another singlet at δ 8.69 ppm corresponds to quinoline singlet, it is also integrated for one proton. The morpholine protons were showed in between δ 3.43-3.93 ppm as two triplets and reaming all protons were shown in aromatic region.

¹³C-NMR spectra of the ligand show signal at δ 159.8 ppm assigned to azomethine carbon and the entire signals were as follows: δ 51.4, 66.9, 116.2, 122.5, 122.8, 124.9, 125.2, 127.5, 128.5, 130.7, 137.8, 147.8, 155.0, 155.1.

UV- Vis Spectra and Magnetic moments: The UV-Vis spectra of Schiff base ligand and its metal complexes were recorded in DMSO at room temperature. The absorption bands of a ligand were observed at 275 and 367 nm which correspond to π- π*(- C=C) and n- π*(-C=N) transitions respectively.

In addition, the copper complex displayed absorption band in the range of 440-460 nm, the transition may correspond to the d-d transition of ²B_{1g} → ²A_{1g}, suggesting the complex compatible with square planar geometry.

Table 1
Elemental analysis of Ligand and metal complexes

Compound	M. F.	M.W.	Anal. (%) (found (%))			
			C	H	N	M
Ligand	C ₂₀ H ₁₉ N ₃ O ₂	333	72.05 (72.11)	5.74 (5.68)	12.60 (12.57)	-
[Cu(L)Cl ₂]	C ₂₀ H ₁₉ Cl ₂ CuN ₃ O ₂	467	51.46 (51.39)	3.89 (3.84)	9.00 (8.92)	13.61 (13.63)
[Co(L)Cl ₂]	C ₂₀ H ₁₉ Cl ₂ CoN ₃ O ₂	463	51.97 (51.89)	3.93 (3.84)	9.09 (8.99)	12.75 (12.68)
[Ni(L)Cl ₂]	C ₂₀ H ₁₉ Cl ₂ CuN ₃ O ₂	462	52.00 (51.97)	3.93 (3.88)	9.10 (9.02)	12.70 (12.71)
[Mn(L)Cl ₂]	C ₂₀ H ₁₉ Cl ₂ MnN ₃ O ₂	459	52.42 (52.39)	3.96 (3.89)	9.17 (9.09)	11.99 (12.02)
[Zn(L)Cl ₂]	C ₂₀ H ₁₉ Cl ₂ ZnN ₃ O ₂	469	51.26 (51.23)	3.87 (3.80)	8.97 (8.92)	13.95 (13.91)

Table 2
Mass values of the Ligand and metal complexes.

Compound	Calculated mass	Obtained mass
Ligand	333	334 [M+1] ⁺
Cu(II) complex	467	467 [M] ⁺
Co(II) complex	463	463 [M] ⁺
Ni(II) complex	462	463[M+1] ⁺
Mn (II) complex	459	460 [M+1] ⁺
Zn(II) complex	469	469 [M] ⁺

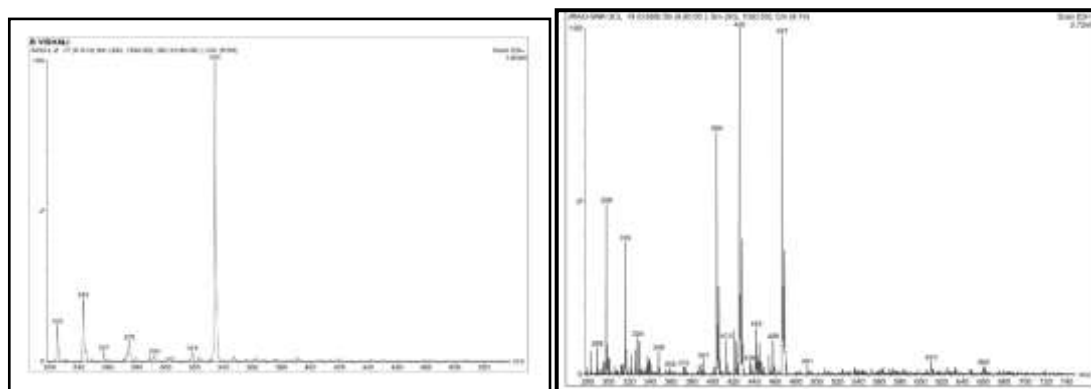


Figure 1: Mass spectrum of ligand and Cu(II) complex.

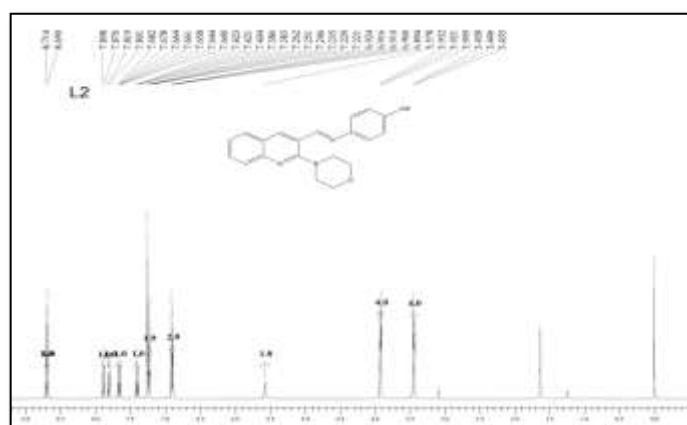


Figure 2: ¹H-NMR spectrum of ligand

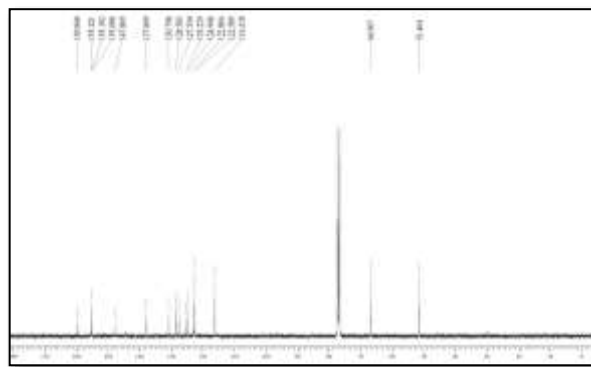
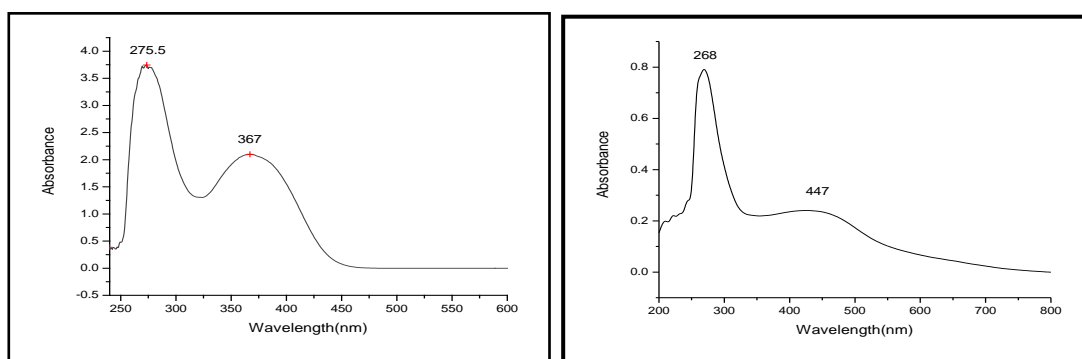
Figure 3: ^{13}C -NMR spectrum of ligand

Figure 4: UV-Vis spectra of ligand and Cu(II) complex

Table 3
UV spectrums values of the ligand & metal complexes.

Compound	Wavelength (nm)
Ligand	275, 367
Cu(II) complex	268, 447
Co(II) complex	260, 312, 428, 630-655
Ni(II) complex	259, 295, 462
Zn(II) complex	260, 390-456(LMCT)
Mn(II) complex	259, 299, 440

The cobalt complex showed the absorption bands in the range 428 nm corresponding to the d-d transition $^4\text{A}_2(\text{F}) \rightarrow ^4\text{T}_1(\text{P})$, this complex also showed another band in the range of 630-655 nm assigned to the $^4\text{A}_2(\text{F}) \rightarrow ^4\text{T}_1(\text{F})$ transition, suggesting that the complex is compatible with tetrahedral geometry. Nickel complex showed a medium intensity band in the range 462 nm suggesting that the complex is compatible with square planar geometry. The zinc complex showed broad band in the range of 390-456 nm due to ligand to metal charge transfer transition suggesting that the geometry of the complex was Tetrahedral.

Manganese complex displayed the absorption band in the range of 400-480 nm, the transition may correspond to the d-d transition $^6\text{A}_1 \rightarrow ^4\text{T}_2(\text{G})$ and $^6\text{A}_1 \rightarrow ^4\text{T}_1(\text{G})$ suggesting that the complex is compatible with tetrahedral geometry. The complexes Cu(II), Co(II) and Mn(II) showed magnetic moment values at 1.82 B.M., 4.38 B.M and, 5.77 B.M. respectively the values are also supported by the electronic spectral data also. The complexes Ni(II) and Zn(II) do not

show any magnetic moment value and it was suggested that the complexes are diamagnetic property.

Infrared spectroscopy: A strong band at 1619 cm^{-1} was assigned to the Azomethine nitrogen of the ligand which was shifted to another frequency in the corresponding metal complexes. The frequencies of Cu(II), Co(II) Ni(II), Mn(II) and Zn(II) complexes were observed at 1592, 1594, 1590, 1601 and 1589 cm^{-1} respectively. This confirms the coordination of azomethine nitrogen to the metal ion. The broad peak around $3100\text{--}3500\text{ cm}^{-1}$ indicates the presence of water molecules. The presence of oxygen and nitrogen in the coordination sphere is further confirmed by the presence of (M–N) and (M–O) bands at $400\text{--}600\text{ cm}^{-1}$ regions. The FTIR results show that all Schiff base ligand act as tridentate chelating ligand.

Thermal analysis: It is observed that all the metal complexes did not show any significant weight loss up to 200°C suggesting the absence of water molecules. All the

complexes show significant weight loss in between 400-800 °C due to removal of organic moiety. The thermo gram above this temperature gave a straight line indicating the formation of metal oxide.

The ligand and metal complexes composition were obtained from Energy Dispersive X-ray (EDX) analysis. The analysis of ligand and Cu(II) complex is represented in figure 7, it is

observed that the experimental atom percentage is close to the expected (theoretical) values. In EDX spectrum-1 the ligand shows three characteristics signals which correspond to C (carbon), O (Oxygen) and N (nitrogen); it indicates the ligand present without any impurity; in spectrum-2 the Cu complex shows C, O, N with Cu and Cl characteristics signals, it clearly confirms the formation of $[\text{Cu}(\text{L})\text{Cl}_2]$ complex.

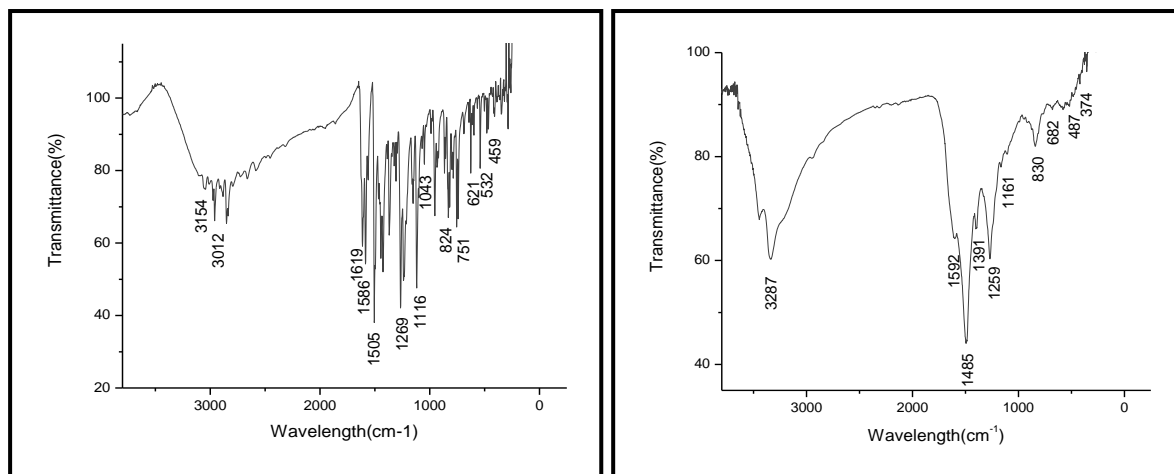


Figure 5: FT-IR spectrums of ligand and Cu(II) complex

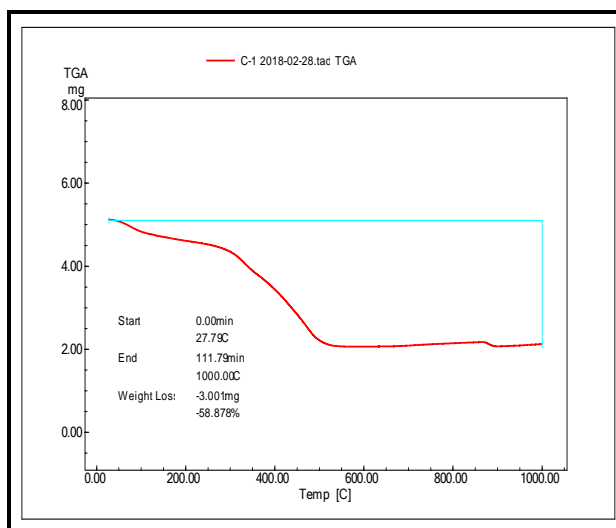


Figure 6: TG curve of the Cu(II) complex

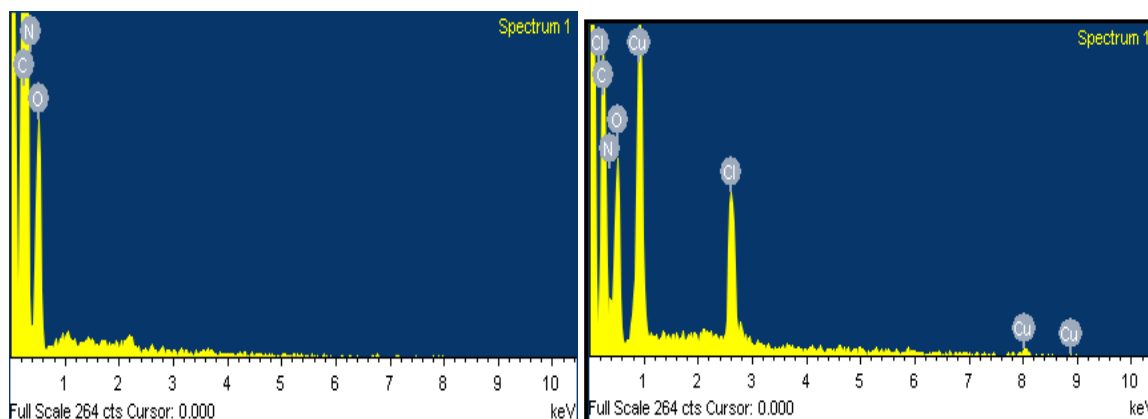


Figure 7: EDX images of the ligand and Cu(II) complexes

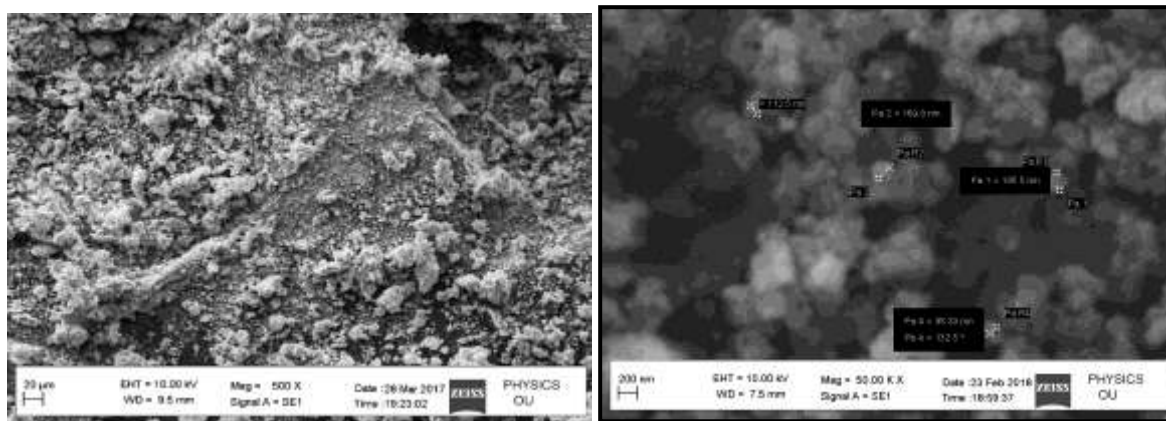


Figure 8: SEM images of the ligand and Cu (II) complexes

Table 4
Antimicrobial zone of inhibition for ligand and their metal complexes:

Compound	<i>Bacillus faecalis</i>	<i>Staphylococcus aureus</i>	<i>Klebsiella pneumoniae</i>	<i>Escherichia coli</i>	<i>A. Niger</i>	<i>F. Oxysporum</i>
Ligand	05	06	06	08	05	07
Cu(II)	16	22	21	21	10	11
Co(II)	17	09	07	19	08	07
Ni(II)	21	19	14	24	07	14
Zn(II)	10	04	09	07	08	08
Mn(II)	09	19	23	13	05	08
Ampicillin	30	28	35	32	---	---
Grieseofulvin	---	---	---	---	13	18

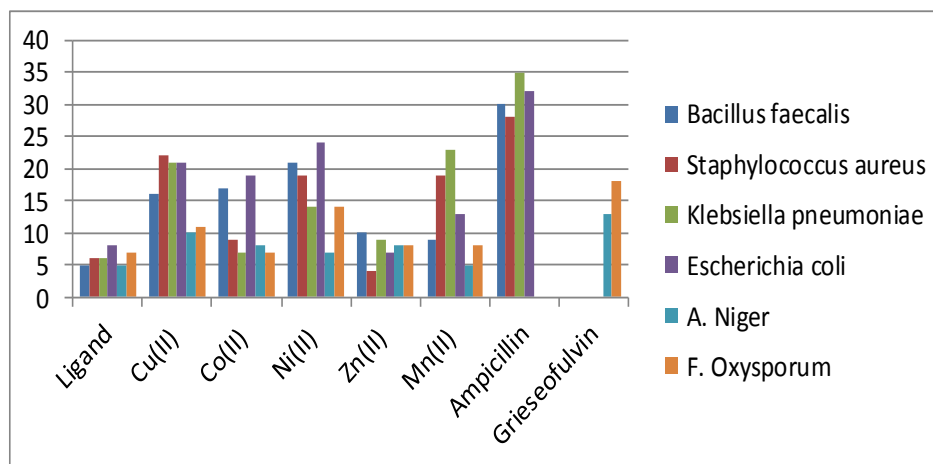


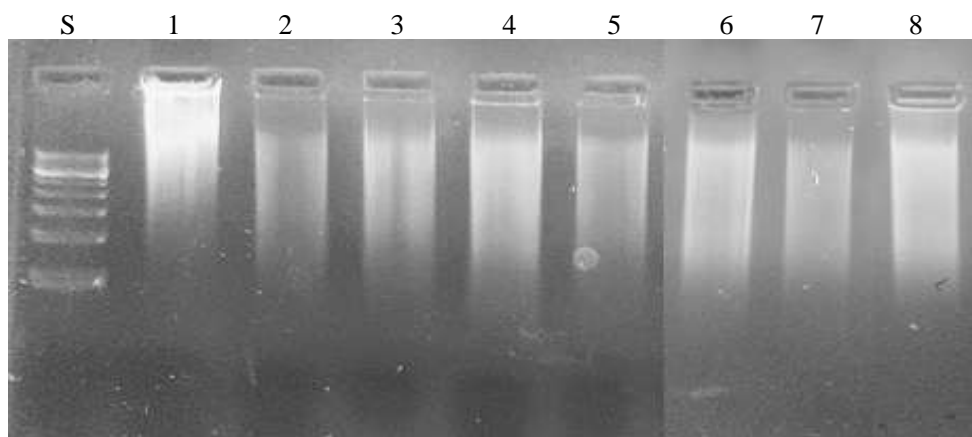
Figure 9: Graphical representation of Antimicrobial activity of the ligand and their metal complexes:

The SEM (Scanning Electron Microscope) is used to evaluate the morphology and particle size of the compounds. The SEM photographs of Ligand and Cu complex are shown in figure 8. The SEM micrographs show the agglomerate particles of the complexes. In case of ligand and Cu complex, some agglomerates appear to have tiny needles, while the other agglomerates appear to be of spherical plates like morphologies.

Antimicrobial activity: The antimicrobial activity zone of inhibition of the Schiff base ligand and its metal complexes values are tabulated in the table 4. It is observed that all the

metal complexes have shown greater activity than free ligand. This is explained on the basis of chelation theory and overtones concept. The complexes have shown good activity against all microorganisms compared with slandered drug.

The antimicrobial screening results suggested that most of the metal complexes showed better activity compared to their Schiff base. Order of the antibacterial activity of complexes was shown as follows as Ni>Co>Cu>Zn>Mn for *Bacillus faecalis*, Cu>Ni>Mn>Co>Zn for *Staphylococcus aureus*, Mn>Cu>Ni>Zn>Co for *Klebsiella pneumoniae* and Ni>Cu>Co>Mn>Zn>for *Escherichia coli*.



Lane-S: DNA+Marker; Lane-1: Control DNA; Lane-2: Control DNA+DMSO; Lane-3: DNA+Cu(II) complex+H₂O₂; Lane-4: DNA+Co(II) complex+H₂O₂; Lane-5: DNA+ Ni(II) complex+H₂O₂; Lane-6: DNA+Zn(II) complex+H₂O₂; Lane-7: DNA+Mn(II) complex+H₂O₂; Lane-8: DNA+ligand+H₂O₂

Figure 10: DNA cleavage of ligand and their metal complexes:

Order of the antifungal activity of complexes was shown as follows as Cu>Co>Zn>Ni>Mn for *Aspergillus Niger* and Ni>Cu>Mn>Zn>Co for *Fusarium Oxysporum*.

DNA cleavage: From the figure 10, it is concluded that few complexes exhibited nuclease activity in the presence of H₂O₂. The control (CT-DNA) alone does not show any cleavage activity. The complete cleavage of DNA observed with the nickel and manganese complexes, partial cleavage of DNA was observed with copper complex, no cleavage of DNA was observed with ligand, cobalt and zinc metal complexes.

Acknowledgement

The authors are thankful to the Head, Department of Chemistry for providing laboratory facilities. The authors are also thankful to the Director, Central Facilities for Research and Development (CFRD), Osmania University for providing IR and NMR spectral analysis. The author AK was thankful to the CSIR, New Delhi, for providing financial support.

References

1. Shah N.K., Shah N.M., Patel M.P. and Patel R.G., *Chin. Chem. Lett.*, **23**, 454 (2012)
2. Zieba A., Sochanik A., Szurko A., Rams M., Mrozek A. and Cmoch P., *Eur. J. Med. Chem.*, **45**, 4733 (2010)
3. Carta A., Palomba M., Briguglio I., Corona P., Piras S., Jabes D., Guglierame P., Mollicotti P. and Zanetti S., *Eur. J. Med. Chem.*, **46**, 320 (2011)
4. Dominguez J.N., Gamboa N., Rodrigues J.R. and Angel J.E., *Lett. Drug Design Discov.*, **4**, 49 (2007)

5. Abdou W.M., Khidre R.E. and Kamel A.A., *Arch. Pharm. Chem. Life Sci.*, **345**, 123 (2012)
6. Bawa S. and Kumar S., *Indian J. Chem.*, **48B**, 142 (2009)
7. Kouznetsov V.V., Méndez L.Y.V., Leal S.M. and Cruz U.M., *Lett. Drug Design Discov.*, **4**, 293 (2007)
8. Luo Z.G., Zeng C.C., Yang L.F., He H.Q., Wang C.X. and Hu L.M., *Chin. Chem. Lett.*, **20**, 789 (2009)
9. Wu Q. L., Li Y.Q., Yang X.L. and Ling Y., *Chin. J. Org. Chem.*, **32**, 747 (2012)
10. Sashidhara K.V., Kumar A., Bhatia G., Khan M.M., Khanna A.K. and Saxena J.K., *Eur. J. Med. Chem.*, **44**, 1813 (2009)
11. Malik M.A., Wani M.Y., Al-Thabaiti S.A. and Shiekh R.A., *J. Incl. Phenom. Macro.*, **78(1-4)**, 15, (2013)
12. Bhaskar V.H. and Mohite P.B., *J. Optoelectron. Biomed. Mat.*, **2**, 249 (2010)
13. El-Sayed W.A., El-Kosy S.M., Ali O.M., Emselm H.M. and Abdel-Rahman A.A.H., *Acta Pol. Pharm.*, **69**, 669 (2012)
14. Vigato P.A. and Tamburini S., *Coord. Chem. Rev.*, **248**, 1717 (2004)
15. Adams M., Li Y., Khot H., Kock De C., Smith P.J., Land K., Chibale K. and Smith G.S., *Dalton Trans.*, **42**, 4677 (2013)
16. Bhat M.A., Al-Omar M.A. and Siddiqui N., *Med. Chem. Res.*, **9**, 4455 (2013).

(Received 02nd December 2019, accepted 27th February 2020)